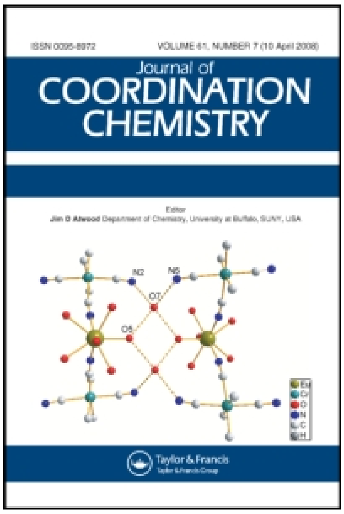

Journal of Coordination Chemistry

Publication details, including instructions for authors and subscription information:
http://www.informaworld.com/smpp/title~content=t713455674

Kinetic and characterization studies of iron(II) and iron(III) complex formation reactions with hydrazinopyridine

Ahmed A. Soliman[a]; Mohamed M. Khattab[b]; Wolfgang Linert[c]
[a] Faculty of Science, Department of Chemistry, Cairo University, Giza, Egypt [b] Faculty of Science, Department of Chemistry, UAE University, Al-Ain, UAE [c] Institute of Applied Synthetic Chemistry, Vienna University of Technology, Getreidemarkt 9-163AC, A-1060 Vienna, Austria

To cite this Article Soliman, Ahmed A. , Khattab, Mohamed M. and Linert, Wolfgang(2008) 'Kinetic and characterization studies of iron(II) and iron(III) complex formation reactions with hydrazinopyridine', Journal of Coordination Chemistry, 61: 13, 2017 — 2031

To link to this Article: DOI: 10.1080/00958970701824373

URL: http://dx.doi.org/10.1080/00958970701824373

Journal of Coordination Chemistry
Vol. 61, No. 13, 10 July 2008, 2017–2031

Kinetic and characterization studies of iron(II) and iron(III) complex formation reactions with hydrazinopyridine

AHMED A. SOLIMAN*†, MOHAMED M. KHATTAB‡ and
WOLFGANG LINERT§

†Faculty of Science, Department of Chemistry, Cairo University, Giza, Egypt
‡Faculty of Science, Department of Chemistry, UAE University, Al-Ain, UAE
§Institute of Applied Synthetic Chemistry, Vienna University of Technology,
Getreidemarkt 9-163AC, A-1060 Vienna, Austria

(*Received 4 December 2006; in final form 11 June 2007*)

Reactions of iron(II) and iron(III) with hydrazinopyridine have been investigated. The metal-to-ligand ratio of the two complexes was determined to be 1 : 3 and the stability constants of $[Fe(hypz)_3]^{2+}$ and $[Fe(hypz)_3]^{3+}$ were evaluated as $2.51 \times 10^2\,L^3\,mol^{-3}$ and $1.94 \times 10^3\,L^3\,mol^{-3}$, respectively. The complex formation reactions were studied kinetically as a function of [hzpy] at various temperatures (15–37°C) at fixed pH (7.5) using stopped-flow techniques. Kinetic results suggest that the binding of hzpy with Fe(II) or Fe(III) takes place in two consecutive steps: a slow and [hzpy] dependent rate-determining step followed by [hzpy] independent ring closure. The activation parameters for both steps in the two systems have been calculated. The low $\Delta H_1^{\neq}$ (57 ± 1, $46 \pm 2\,kJ\,mol^{-1}$) as well as $\Delta H_2^{\neq}$ (21 ± 0.1, $21 \pm 0.1\,kJ\,mol^{-1}$) for the first and second steps, respectively, and the large negative values of $\Delta S_1^{\neq}$ (-81 ± 4, $-110 \pm 5\,J\,K^{-1}\,mol^{-1}$) as well as $\Delta S_2^{\neq}$ (-197 ± 3, $-197 \pm 3\,J\,K^{-1}\,mol^{-1}$) for the first and second steps for both Fe(II) and Fe(III) systems, respectively, indicate associative modes of activation for both ligand substitution processes. $[Fe(hypz)_3](PF_6)_2$ and $[Fe(hypz)_3](PF_6)_3$ were isolated as solids and characterized using CHN, IR, magnetic and UV-Visible measurements.

Keywords: Fe(II) complexes; Fe(III) complexes; Hydrazinopyridine; Kinetics; Stability constants

1. Introduction

The role of ligands in coordination and organometallic chemistry does not need emphatic presentation since their fundamental importance in determining the morphology and the chemical–physical properties of the complexes are well documented by a wealth of literature data. Pyridylamines find application in the field of coordination chemistry with different metal ions for their biological,

---

*Corresponding author. Email: ahmedsoliman61@gmail.com

Journal of Coordination Chemistry
ISSN 0095-8972 print/ISSN 1029-0389 online
DOI: 10.1080/00958970701824373

spin transition, organometallic and catalytic activities [1–15]. Hydrazinopyridine (hzpy) is a good ligand for complex formation with metal ions. Very little has been published on this ligand; its structure, which might involve potential anti-tumor properties, encouraged us to study its reaction with different metal ions [16–24]. In this investigation, we report the reaction of hydrazinopyridine with iron(II) and iron(III) in solution and in the solid state.

2. Experimental

2.1. *Materials*

All chemicals used in this study were of the highest purity available. $Fe(ClO_4)_2$, $Fe(NO_3)_3 \cdot 9H_2O$, hydrazinopyridine, KNO_3, hexamine and H_2O_2 were supplied by Aldrich. All solvents were of analytical grade and were purified by distillation before use.

2.2. *Measurements and synthesis of complexes*

Elemental analyses (C, H, N) were performed in the Central Laboratory Unit (CLU) of UAE University; the analyses were repeated twice. The IR spectra have been recorded using a NEXUS 470 FT-IR spectrometer, Thermo Nicolet Corporation, running under the OMNIC software package between 4000–400 cm^{-1}. The spectra are recorded using KBr pellets. UV-Vis measurements were performed with a Cary 50 Conc, VARIAN UV-Vis spectrophotometer, in the wavelength range 200–900 nm. The molar magnetic susceptibilities were measured on powdered samples (Gouy method) using a Sherwood Scientific magnetic susceptibility balance.

2.2.1. Synthesis of $[Fe(hzpy)_3](PF_6)_2$. 0.26 g (1 mmol) of $Fe(ClO_4)_2$ was mixed with 1.01 g (3 mmol) of hydrazinopyridine in 30 mL ethanol. The solution was degassed with nitrogen and 0.34 g (2 mmol) of $NaPF_6$ was added and stirred under nitrogen until the sodium hexafluorophosphate completely dissolved. The mixture was further stirred in the closed reaction flask for two hours and a dark violet precipitate separated. The solid complex was filtered off and washed thoroughly with ethanol, then with diethyl ether and kept under reduced pressure overnight.

2.2.2. Synthesis of $[Fe(hzpy)_3](PF_6)_3$. 0.40 g (1 mmol) of $Fe(NO_3)_3 \cdot 9H_2O$ was mixed with 1.01 g (3 mmol) of hydrazinopyridine in 30 mL ethanol, 0.50 g (3 mmol) of $NaPF_6$ was added and the solution was stirred for two hours where the dark reddish violet precipitate separated. The solid complex was filtered off and washed thoroughly with ethanol, then diethyl ether and kept under vacuum overnight.

2.3. *Determination of the complex formula and evaluation of the stability constants*

The composition and stability constants for both Fe(II) and Fe(III) complexes with hzpy were determined spectroscopically by two different methods.

(a) Limiting logarithmic method

For this method, two sets of solutions were prepared. Set 1: solution mixtures of 0.5 mL of 0.001 M metal solution mixed with 0.25, 0.5, 0.75, 1, 1.25, 1.5, 1.75 and 2 mL of the ligand solution. To each solution, the required amount of KNO_3 was added to obtain $I = 0.1$ M. All solutions were buffered to pH = 7.5 (hexamine buffer), filled to the 10-mL mark, and then placed in a thermostated bath at 25°C for 30 min. The absorbances of the solutions were measured at wavelengths of 562 and 552 nm for Fe(II) and Fe(III) systems, respectively, by UV-Vis (Cary 50 Conc, VARIAN). Set 2 was prepared by the same procedure, but with solutions having a constant ligand concentration (0.5 mL of 0.001 M of ligand solution) and variable metal concentration (0.25–2.0 mL of 0.001 M metal solution).

(a) Turner–Anderson method

This method is based on preparing a number of solutions by mixing variable volumes of Fe(II) or Fe(III) solutions (0.001 M) and hzpy solution (0.001 M). The mixtures were buffered (pH 7.5) and kept in a water bath (at 25°C) for 30 min. The absorbances of all solutions were measured at wavelengths of 562 and 552 nm for Fe(II) and Fe(III), respectively. The experiments were repeated using 0.0005 M solutions of the metal ions and hzpy. For each system continuous variation curves were plotted on the same graph.

2.4. *Kinetic measurements*

2.4.1. Stopped-flow measurements. Solutions of Fe(II) or Fe(III) of constant ionic strength (0.1 M using KNO_3) were mixed with the appropriate ratio with hzpy and buffered to pH 7.5 using hexamine buffer. All solutions were carefully deoxygenated before use and then transferred to the stopped-flow apparatus in sealed syringes. The spectra of free ligand and the complexes were obtained in the wavelength range 200–900 nm. Kinetic stopped-flow measurements in the visible and near UV region were carried out with a high speed Applied Photophysics SX.18 MV-R stopped-flow spectrometer equipped with a diode array detector and a Shimadzu TB thermo-bath (accuracy ±0.1°C) running under the SX.18 MV kinetic package. Rate constant data were measured under pseudo-first-order conditions (20–60 fold excess of the ligand with respect to the metal concentration). Experimentally observed rate constant data (k_{obs}) are an average of six to eight kinetic runs.

3. Results and discussion

3.1. *Characterization of the solid complexes*

Elemental analyses of the isolated complexes are given in table 1 with good agreement between the calculated and experimental values. The IR spectra of hzpy showed

Table 1. Analytical data of hydrazinopyridine and its Fe(II) and Fe(III) complexes.

			CHN, Calcd (found)					UV-Vis (nm)			
Complex	M. Wt. (m/e)	Color	%C	%H	%N	IR bands (cm^{-1})	Magnetic moment μ (BM)	Water	DMSO	Ethanol	Acetonitrile
$[Fe(hzpy)_3] (PF_6)_2$	673.16 (671.20)	Dark violet	25.76 (25.27)	3.14 (2.97)	18.73 (17.99)	3400, 3233 (ν_{NH_2}) 1290, 1089, 841 (ρ_{NH_2}) 623, 483 (py) 506 ($\nu_{M\text{-}N}$)	3.85	381sh 562	391sh 575	379sh 562	377sh 572
$[Fe(hzpy)_3] (PF_6)_3$	818.02 (817.10)	Reddish violet	22.02 (21.89)	2.59 (2.53)	15.41 (15.33)	3414, 3200 (ν_{NH_2}) 1288,1121, 837 (ρ_{NH_2}) 623, 445 (py) 559 ($\nu_{M\text{–}N}$)	1.67	552	555	551	549

IR (hzpy): 3420 b, 3306 b (ν_{NH_2}), 1285, 1020, 769 (ρ_{NH_2}), 608 w, 406 w (py).

medium to strong band(s) at 3420–3363 cm^{-1} and 3308–3287 cm^{-1}, assigned to stretching of the NH_2 group. These bands are shifted to lower frequencies in the spectra of complexes, indicating coordination of these groups to metal ions [25]. The coordination of the NH_2 instead of NH groups is further confirmed from the shifts of their deformation vibrations found at 1285–1207 cm^{-1} ($\rho_t NH_2$), 1150–1048 ($\rho_w NH_2$) and 769–759 ($\rho_r NH_2$) to higher frequencies in the spectra of complexes. The pyridine (py) vibrations at 608 cm^{-1} (in-plane ring deformation) and 406 cm^{-1} (out-of-plane ring deformation) were shifted in the spectra of complexes to higher frequencies at 623 cm^{-1} and 445–483 cm^{-1}, respectively [25].

The spectra of the isolated complexes were measured in different solvents (table 1). UV-Vis spectra of $[Fe(hzpy)_3](PF_6)_2$ displayed two absorption bands at 562–575 nm and 377–391 nm. The latter, found as a shoulder, can be assigned to the n–π^* transition of the ligand which is shifted upon complexation. The 562–575 nm band is assigned to the d–d transition of the octahedral iron; $[Fe(hzpy)_3](PF_6)_3$ displayed a d–d transition band at 549–555 nm.

The magnetic moments are reported in table 1. $[Fe(hzpy)_3](PF_6)_2$ complex has a μ_{eff} value of 3.85 which is associated with a high-spin octahedral geometry, $t_{2g}^4 e_g^2$ [26, 27]; $[Fe(hzpy)_3](PF_6)_3$ has a μ_{eff} of 1.67 which relates to a moment of a single electron, suggesting a low-spin configuration with $t_{2g}^5 e_g^0$. These findings are consistent with ligand field strengths, as the amine ligands are considered to interact with a "strong field" with the trivalent metal ions and with "weak to moderate field" with the bivalent ions [28].

3.2. *UV-Vis spectra in solution*

A series of solutions was made by mixing 0.5 mL of 0.001 M Fe(II) or Fe(III) with 1.5 mL of 0.001 M hzpy at different pH values using hexamine buffer (pH range 3.0–10). The ionic strength of the mixtures was kept constant (0.1 M using KNO_3). The absorbances at 25°C of all solutions were measured at the wavelengths 562 and 552 nm for Fe(II) and Fe(III) systems, respectively, and plotted against the pH values of the measured solutions (figure 1). The pH 7.5 was chosen as an optimum pH value for all consequent UV-Vis spectral studies.

Interactions between Fe(II) or Fe(III) with hzpy showed interesting features (figure 2). The free ligand exhibits two λ_{max} values at 248 and 300 nm, which may be assigned to n–π^* and π–π^* transition within the pyridine, respectively. Upon addition of aqueous solution of Fe(II), new absorption peaks with maxima at 381and 562 nm have been observed, whereas on addition of Fe(III) only one absorption peak was observed at 552 nm. Time-resolved spectra for the reaction of $[Fe^{II/III}]$ $([c]) = 5 \times 10^{-4}$ M and hzpy $([c]) = 5 \times 10^{-3}$ M are given in figures 3 and 4. Repetitive spectral scanning for the Fe(II)-hzpy system at 0.16 s intervals within ca 60 s total time revealed a decrease in the absorbance at 381 nm and increase in absorbance at 562 nm with increasing time (figure 3). Repetitive spectral scanning for the Fe(III)-hzpy system at the same time interval revealed an increase in absorbance at 552 nm (figure 4).

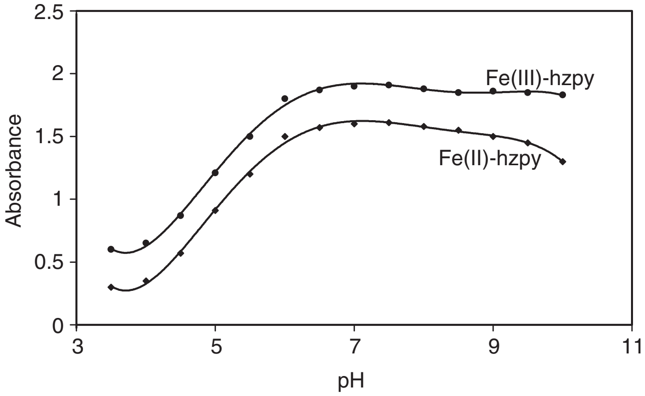

Figure 1. Typical plot of the absorbance of Fe(II)-hzpy and Fe(III)-hzpy systems at different pH. Experimental conditions: 0.1 mmol complex, $I = 0.1$ M and $t = 25°C$. The absorbances of all solutions were measured at wavelengths of 562 and 552 nm for Fe(II) and Fe(III) systems, respectively.

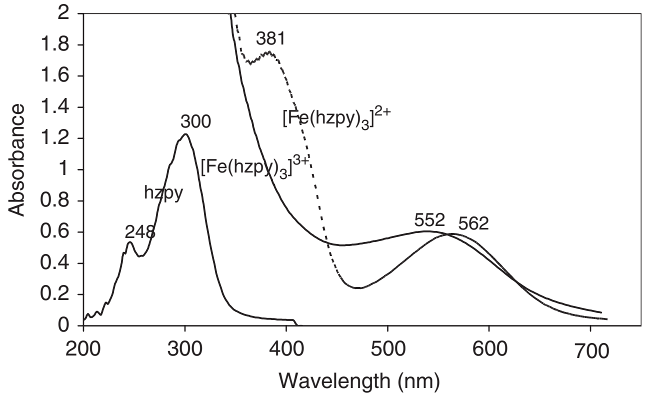

Figure 2. Spectra of free hzpy, $[Fe(hzpy)_3]^{2+}$ and $[Fe(hzpy)_3]^{3+}$ in water at 25°C and pH = 7.5; $[Fe^{II/III}] = 5 \times 10^{-4}$ M and $[hzpy] = 5 \times 10^{-3}$ M.

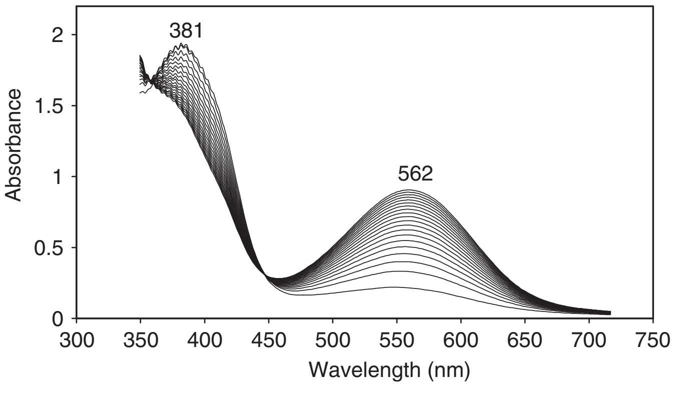

Figure 3. Repetitive-scan spectra at 0.16 s intervals within ca 60 s for the reaction of Fe(II) with hzpy. $[Fe(II)] = 5 \times 10^{-4}$ M; $[hzpy] = 1.5 \times 10^{-3}$ M; pH 7.5; $I = 0.1$M, $t = 25°C$.

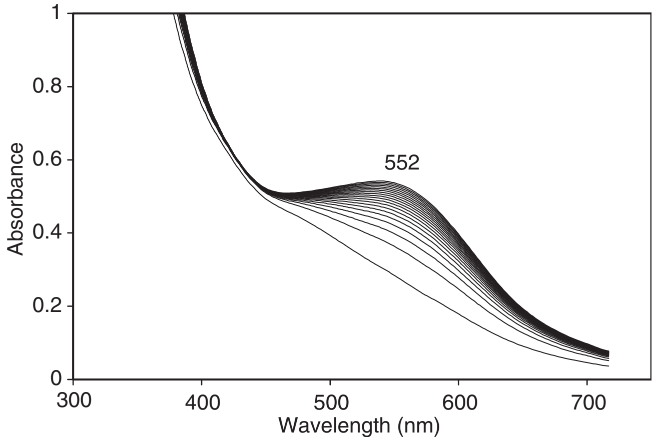

Figure 4. Repetitive-scan spectra at 0.16 s intervals within ca 60 s for the reaction of Fe(II) with hzpy. [Fe(III)] $= 5 \times 10^{-4}$ M; [hzpy] $= 1.5 \times 10^{-3}$ M; pH 7.5; $I = 0.1$M, $t = 25$°C.

3.3. *Composition and stability constants of Fe(II) and Fe(III) with hzpy*

Composition and stability constants of $[Fe(hypz)_3]^{2+}$ and $[Fe(hypz)_3]^{3+}$ were evaluated using the limiting logarithmic method [29]. The method depends on measuring the absorbance of metal and ligand solutions in which the concentrations of the two species are varied at constant total ionic strength of 0.1 M KNO_3 (sets 1 and 2, experimental part). It is assumed that Beer's law is applicable within the working range and that the maximum absorption is proportional to the concentration of the complex, i.e. ($\log A$ *vs.* $\log[M_mL_l]$).

For the reaction

$$m\mathrm{M} + l\mathrm{L} \Leftrightarrow \mathrm{M}_m L_l \tag{1}$$

the stability constant K is given by

$$\mathrm{K} = \frac{[M_mL_l]}{[M]^m[L]^l} \tag{2}$$

By taking logarithm of equation (2)

$$\log[M_mL_t] = m\log[M] + l\log[L] + \log K \tag{3}$$

the values for m and l could be found by plotting ($\log \mathrm{A}$ *vs.* $\log[M]$ and ($\log A$ *vs.* $\log[L]$), respectively, for the two sets of solutions in which one set has constant metal and variable ligand concentration and the other set has constant ligand and variable metal concentration (figure 5). Both $\log[M]$ and $\log[L]$ refer to the free metal and ligand concentration which could be evaluated by subtracting the amount of metal or ligand bound as $[M_mL_l]$ calculated at the peak absorption curves ($\varepsilon = 750\,\mathrm{M^{-1}\,cm^{-1}}$ at $\lambda = 562$ nm and $\varepsilon = 762\,\mathrm{M^{-1}\,cm^{-1}}$ at $\lambda = 552$ nm for $[Fe(hypz)_3]^{2+}$ and $[Fe(hypz)_3]^{3+}$ complexes, respectively) from the total metal or ligand concentration. The slope of the curve in case I gives "l" while that in case II gives "m" so that K and the composition of the complex can be evaluated.

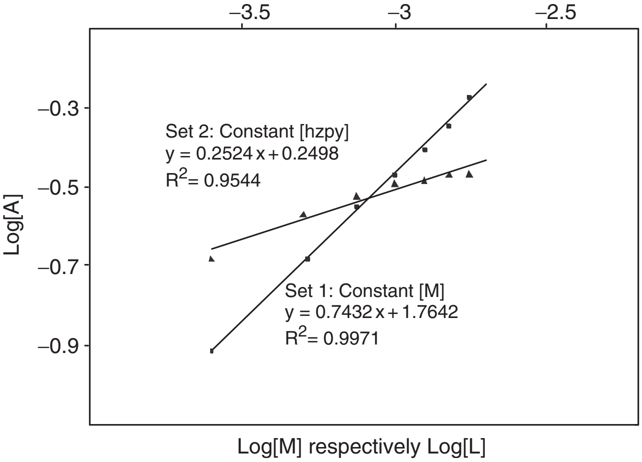

Figure 5. The limiting logarithmic method. Set I at constant [Fe(II)] of 0.001 M and Set II at constant [hzpy] of 0.001 M.

The slope for set I was found to be $l = 0.743$, and that of the second set $m = 0.253$. Therefore, the composition of the complex $= lm = 2.94 \cong 3$ suggesting a *tris* complex species ML_3 ($[Fe(hzpy)_3]^{2+}$). Accordingly, log K was found to equal 2.33 and hence $K = 2.14 \times 10^2\ L^3\,mol^{-3}$.

The stability constant and the composition of the complex were re-determined using the Turner–Anderson method [30], which consists of plotting two continuous variation curves for a given range of compositions using two different concentrations (0.001 M and 0.0005 M). If the initial concentrations of metal ion and ligand are a and b, respectively, then

$$K = \frac{x}{(a - x)(b - x)} \tag{4}$$

where K is the stability constant and x is the concentration of the complex. Therefore, for any two solutions on the two curves with the same optical density,

$$K = \frac{x}{(a_1 - x)(b_1 - x)} = \frac{x}{(a_2 - x)(b_2 - x)} \tag{5}$$

where subscripts 1 and 2 refer to reagent concentrations. Selecting two sets from the graphs representing $a_1 = 1.6 \times 10^{-4}$, $b_1 = 4.0 \times 10^{-4}$ M and $a_2 = 5.0 \times 10^{-5}$, $b_2 = 5.0 \times 10^{-5}$ M figure 6 is obtained. With this the stability constant (K) of $[Fe(hzpy)_3]^{2+}$ complex was evaluated; $K = 2.51 \times 10^2\,L^3\,mol^{-3}$ is in good agreement with the previous value resulting from the limiting logarithmic method. It can be seen from the figure that the composition of the complex ML_n is $n = X_L/X_M = 3.1$, confirming the 1 : 3 (M : L) complex species.

The composition and stability constant of Fe(III)-hzpy system were evaluated by the same way as Fe(II)-hzpy system. The composition was set as ML_3 with stability constant equal to $K = 1.94 \times 10^3\ L^3\,mol^{-3}$.

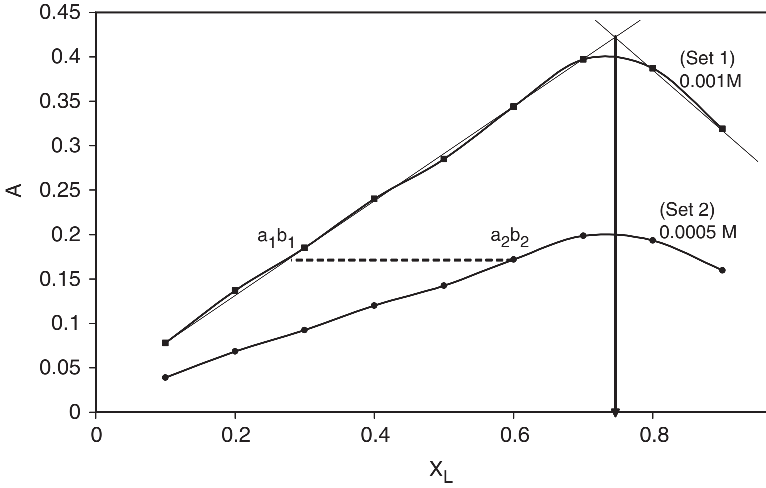

Figure 6. Turner–Aanderson method: continuous variation curves for Fe(II)-hzpy system.

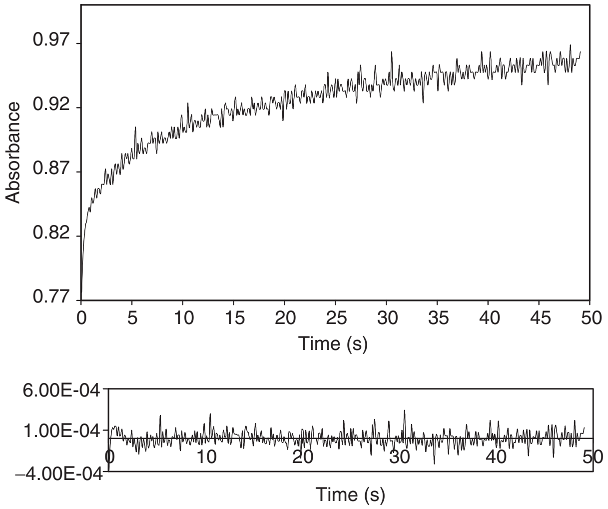

Figure 7. Typical kinetic trace for reaction between Fe(II) (5×10^{-4} M) and hzpy (1.5×10^{-3} M) at pH 7.5, $I = 0.1$M and $t = 25°$C. The trace was fitted to double exponentials by following the growth in the absorbance at 562 nm. The lower trace represents the difference between the experimental and calculated curves.

3.4. *Kinetic investigations*

The reactions of Fe(II) and Fe(III) with hzpy were followed under pseudo-first-order conditions using an excess (20–60-fold) of the nucleophile over the metal ions to ensure complete reaction. The reaction traces for both systems showed a bi-exponential growth with time (figures 7 and 8). The pseudo-first-order rate constants were extracted by fitting the kinetic traces for both systems to equation (6) [31]:

$$A_t = a_i \exp -k_{\mathrm{obs}}(i)t + a_j \exp -k_{\mathrm{obs}}(j)t + A_\alpha \quad (6)$$

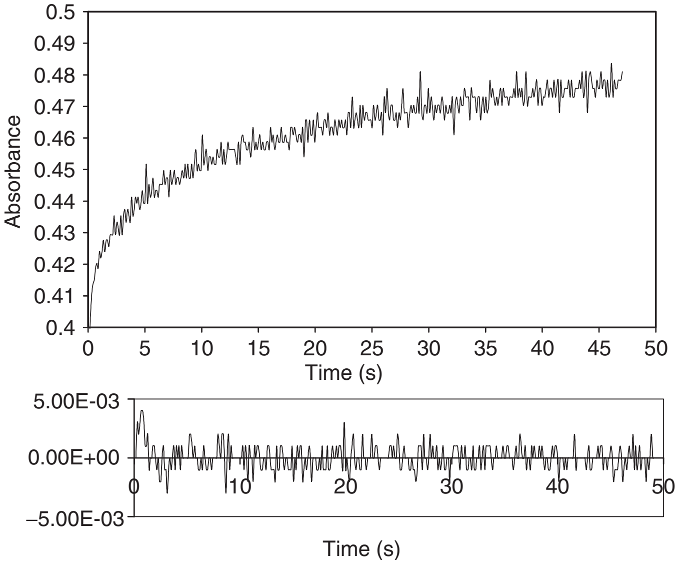

Figure 8. Typical kinetic trace for reaction between Fe(III) (5×10^{-4} M) and hzpy (1.5×10^{-3} M) at pH 7.5, $I = 0.1$M and $t = 25$°C. The trace was fitted to double exponentials by following the growth in the absorbance at 552 nm. The lower trace represents the difference between the experimental and calculated curves.

Table 2. Values of observed pseudo-first-order rate constants for the reaction of Fe(II) and Fe(III) with hzpy at different temperatures, pH 7.5, $I = 0.1$M and $[\mathrm{Fe}^{\mathrm{II/III}}] = 5 \times 10^{-4}$ M.

		Fe(II)		Fe(III)	
t (°C)	[hzpy]	k_{obs1} (s^{-1})	k_{obs2} (s^{-1})	k_{obs1} (s^{-1})	k_{obs2} (s^{-1})
15	0.010	0.32	0.06	0.73	0.10
	0.015	0.34	0.06	1.00	0.13
	0.025	0.40	0.05	1.30	0.09
	0.030	0.45	0.05	1.60	0.11
25	0.010	0.46	0.11	1.11	0.19
	0.015	0.54	0.09	1.37	0.16
	0.025	0.68	0.10	1.72	0.18
	0.030	0.74	0.10	2.00	0.17
37	0.010	0.60	0.11	1.31	0.21
	0.015	0.71	0.12	1.72	0.23
	0.025	0.90	0.12	2.00	0.23
	0.030	1.12	0.10	2.23	0.23

The terms a_i and a_j are the changes in absorbance and $k_{\mathrm{obs}}(i)$ and $k_{\mathrm{obs}}(j)$ are the pseudo-first-order rate constants for the reactions. The k_{obs} values were evaluated by stopped flow technique as an average of six to eight reaction traces at a particular concentration of nucleophile, within an error limit ±5.0%. k_{obs} values were determined from $\log(A_t - A_\alpha)$ *versus* time plots using conventional UV-Vis spectrophotometry. The k_{obs} values are the average of triplicate runs. All k_{obs} values as a function of [hzpy] are listed in table 2.

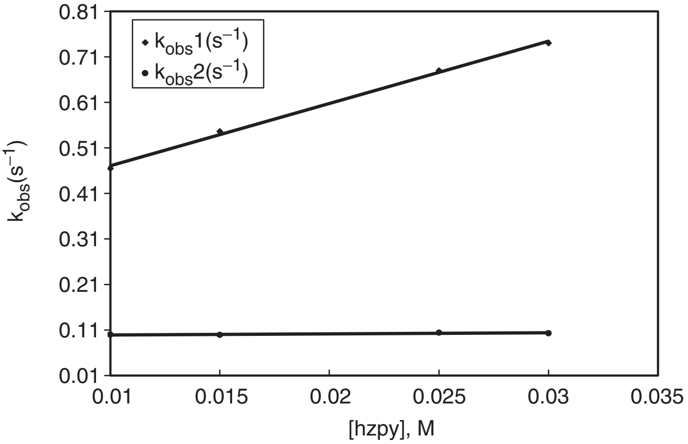

Figure 9. Plot of k_{obs} *vs.* [hzpy] for reaction of Fe(II) with hzpy at pH 7.5, $I = 0.1M$ and $t = 25°C$. $[Fe(II)] = 5 \times 10^{-4}$ M.

3.4.1. Reaction of Fe(II) and Fe(III) with hzpy. The formation reaction of both $[Fe(hzpy)_3]^{2+}$ and $[Fe(hzpy)_3]^{3+}$ involves a consecutive three-step mechanism.

$$[Fe^{II}(H_2O)_6] + hzpy \underset{k-1}{\overset{k_1}{\rightleftarrows}} [Fe^{II}(hzpy)(H_2O)_4]^{2+} + 2H_2O \text{ (very fast)} \qquad (7)$$

$$[Fe^{II}(hzpy)(H_2O)_4]^{2+} + hzpy \underset{k-2}{\overset{k_2}{\rightleftarrows}} [Fe^{II}(hzpy)_2(H_2O)_2]^{2+} + 2H_2O \text{ (very fast)} \qquad (8)$$

$$[Fe^{II}(hzpy)_2(H_2O)_2]^{2+} + hzpy \underset{k_r}{\overset{k_f}{\rightleftarrows}} [Fe^{II}(hzpy)_2(hzpy\text{–}N)(H_2O)]^{2+} + H_2O \text{ (slow)} \qquad (9)$$

$$\text{Ring closure} \Big\downarrow \text{(very slow)}$$

$$[Fe^{II}(hzpy)_2(hzpy\text{–}N,N)]^{2+} + H_2O$$

The kinetic investigation of these reactions show that $\upsilon_1 \gg \upsilon_{-1}$ and $\upsilon_2 \gg \upsilon_{-2}$. Because of the relative magnitudes of these reaction rates, the overall reaction goes very fast to completion. The fastness of the first two steps is shown from the large and fast absorbance changes at the start of the reactions (figures 7 and 8). This could not be followed in figures 3 and 4 which have been collected over 60 s starting from 0.16 s which seems to lie above the time needed for these fast reactions. The steric hindrance caused by the first and second substitution processes of the two hzpy ligands probably accounts for the slowness of the third step, *i.e.* υ_1 and $\upsilon_2 \gg \upsilon_3$, so a sensible approximation is to ignore the back reactions and model the

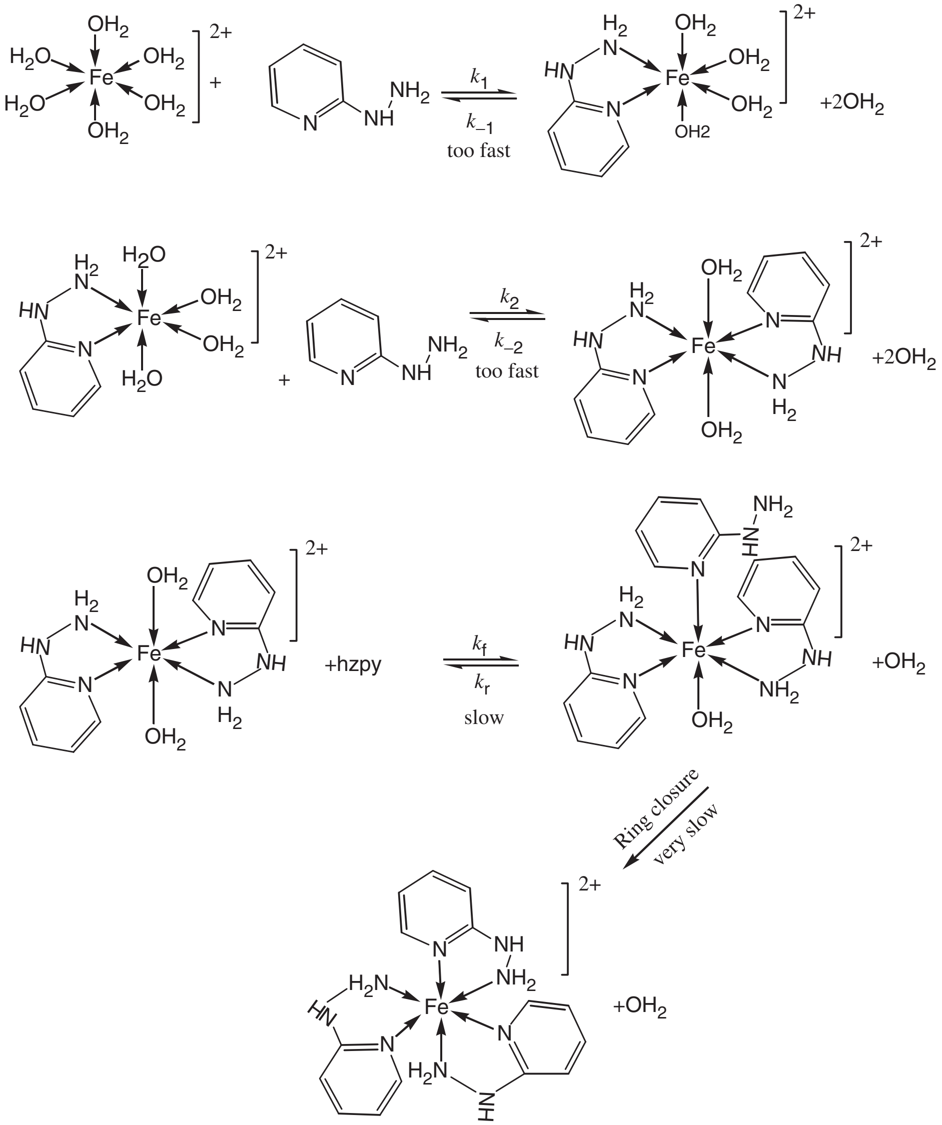

Scheme 1. Schematic representation of the reaction of Fe(II) with hzpy.

Table 3. Rate constants for reaction of Fe(II) and Fe(III) with hzpy at different temperatures, pH = 7.5, $I = 0.1$M and $[Fe^{II/III}] = 5 \times 10^{-4}$ M.

	Fe(II)		Fe(III)	
t (°C)	k_f ($M^{-1} s^{-1}$)	k_r (s^{-1})	k_f ($M^{-1} s^{-1}$)	k_r (s^{-1})
15	6 ± 0.1	0.3 ± 0.2	39 ± 1.0	0.4 ± 0.0
25	14 ± 0.1	0.3 ± 0.0	43 ± 2	0.7 ± 0.0
37	25 ± 0.2	0.4 ± 0.1	47 ± 2	0.9 ± 0.3

Table 4. Comparison between the activation parameters for Fe(II) and Fe(III) systems.

Systems	$\Delta H_1^{\neq}$ (kJ mol^{-1})	$\Delta S_1^{\neq}$ (J K^{-1} mol^{-1})	$\Delta H_2^{\neq}$ (kJ mol^{-1})	$\Delta H_2^{\neq}$ (J K^{-1} mol^{-1})
Fe(II)	57 ± 1	-81 ± 4	21 ± 0.1	-197 ± 3
Fe(III)	46 ± 2	-110 ± 5	21 ± 0.1	-197 ± 3

mechanism of the first two reactions using two irreversible steps while the third is reversible step, or

$$\text{Fe(II)} + \text{hzpy} \xrightarrow{k_1} \text{Fe-(hzpy)} + \text{hzpy} \xrightarrow{k_2} \text{Fe-(hzpy)}_2 + \text{hzpy} \underset{k_r}{\overset{k_r}{\leftrightarrows}} \text{Fe-(hzpy)}_3$$

If one step in this reaction mechanism is much slower than the other, the slow step effectively controls the overall reaction rate. In the present study the first two steps are much faster than the third, so the third step is rate determining. In this particular case, the rate of overall reaction will be given by the rate of the rate-determining step, and the kinetic behavior of the present systems can be rationalized in terms of the following rate expression (equation (10)).

$$k_{\text{obs}} = k_{\text{f}}[\text{hzpy}] + k_{\text{r}} \tag{10}$$

Depending on the above assumption, the kinetic traces (growth at 562 nm and 552 nm) for both Fe(II) and Fe(III) systems, respectively, shown in figures 7 and 8, were found to be double exponential. The values of the observed rate constants (k_{obs1}) corresponding to the primary step in the third substitution process (slow step) involving the coordination of the third hzpy ligand through N atom of the pyridine moiety, exhibited linear dependence on the [hzpy] with an appropriate intercept (figure 9), suggesting operation of the reverse reaction. The rate constant values (k_{obs2}) involving coordination of exocyclic –NH_2 group of hzpy to Fe(II) and Fe(III) centers by dislodging the sixth coordinated water, showed no dependence on the nucleophilic concentration. Scheme 1 is suggested.

As indicated in equation (10), plots of k_{obs} *versus* [hzpy] were linear, as shown in figure 9. The values of k_{f} and k_{r} determined from the slopes and intercepts of such plots are summarized in table 3, k_{f} values were evaluated as $43 \pm 2\,\text{M}^{-1}\,\text{s}^{-1}$ and $14 \pm 0.1\,\text{M}^{-1}\,\text{s}^{-1}$ for Fe(III) and Fe(II) systems, respectively, at 25°C, indicating that Fe(III) reacts with hzpy about 3 times faster than Fe(II).

3.4.2. Effect of temperature on reaction rates. The values of $\Delta H^{\neq}$ and $\Delta S^{\neq}$, determined from Eyring's equation [32], are listed in table 3. The obtained activation parameters ($\Delta H_1^{\neq} = 57 \pm 1\,\text{kJ mol}^{-1}$, $\Delta S_1^{\neq} = -81 \pm 4\,\text{J K}^{-1}\,\text{mol}^{-1}$), ($\Delta H_1^{\neq} = 21.0 \pm 0.1\,\text{kJ mol}^{-1}$, $\Delta S_1^{\neq} = -197 \pm 3\,\text{J K}^{-1}\,\text{mol}^{-1}$) and ($\Delta H_1^{\neq} = 46 \pm 2\,\text{kJ mol}^{-1}$, $\Delta S_2^{\neq} = -110 \pm 5\,\text{J K}^{-1}\,\text{mol}^{-1}$), ($\Delta H_2^{\neq} = 21.0 \pm 0.1\,\text{kJ mol}^{-1}$, $\Delta S_2^{\neq} = -197 \pm 3\,\text{J K}^{-1}\,\text{mol}^{-1}$) for the first step and second step in the Fe(II)-hzpy and Fe(III)-hzpy systems, respectively, are listed in table 4. These values suggest an associative mode of activation for substitution. The low $\Delta H^{\neq}$ values imply a pronounced degree of ligand participation in the transition state and the negative entropy of activation implies increased ordering.

This can be explained by formation of three five-member rings due to participation of exocyclic NH_2 in the coordination.

4. Conclusions

Fe(II) and Fe(III) react with hydrazinopyridine (hzpy) to form stable complexes, $[Fe(hzpy)_3]^{2+}$ and $[Fe(hzpy)_3]^{3+}$. During complex formation, there was no evidence for reduction of Fe(III) to Fe(II) by hzpy. The rate constant values (k_f) and the activation parameters ($\Delta H^{\neq}$ and $\Delta S^{\neq}$) listed in tables 3 and 4 suggest that Fe(III) reacts faster and forms more stable complex than Fe(II). This is also supported by the higher stability constants of $[Fe(hzpy)_3]^{3+}$ over that of $[Fe(hzpy)_3]^{2+}$.

Acknowledgements

Thanks for the financial support is due to the ‘‘Fonds Zur Förderung der Wissenschaftlichen Forschung in Österreich’’ (Project 19335-N17) and to the ‘‘Hochschuljubiläumstiftung der Stadt Wien’’ (Project H-01684/2007).

References

[1] S.K. Padhi. *Thermochim. Acta*, **448**, 1 (2006).
[2] B. Macías, M.V. Villa, M. Salgado, J. Borrás, M. González-Álvarez, F. Sanz. *Inorg. Chim. Acta*, **359**, 1465 (2006).
[3] S. Mundwiler, R. Waibel, B. Spingler, S. Kunze, R. Alberto. *Nucl. Med. Biol.*, **32**, 473 (2005).
[4] C. Müller, C. Dumas, U. Hoffmann, P.A. Schubiger, R. Schibli. *J. Organomet. Chem.*, **689**, 4712 (2004).
[5] A. Mokhir, R. Stiebing, R. Kraemer. *Bioorg. Med. Chem. Lett.*, **13**, 1399 (2003).
[6] G. Baranovi. *Chem. Phys. Lett.*, **369**, 668 (2003).
[7] M. Machuqueiro, T. Darbre. *J. Inorg. Biochem.*, **94**, 193 (2003).
[8] D. Choquesillo-Lazarte, B. Covelo, J.M. González-Pérez, A. Castiñeiras, J.N. Gutiérrez. *Polyhedron*, **21**, 1485 (2002).
[9] U. Brand, H. Vahrenkamp. *Inorg. Chim. Acta*, **308**, 97 (2000).
[10] C. Stern, F. Franceschi, E. Solari, C. Floriani, N. Re, R. Scopelliti. *J. Organomet. Chem.*, **593–594**, 86 (2000).
[11] H. Chaouk, M.T.W. Hearn. *J. Chromatogr. A*, **852**, 105 (1999).
[12] Y. Gultneh, A.R. Khan, D. Blaise, S. Chaudhry, B. Ahvazi, B.B. Marvey, R.J. Butcher. *J. Inorg. Biochem.*, **75**, 7 (1999).
[13] S. Tachiyashiki, K. Mizumachi. *Coord. Chem. Rev.*, **132**, 113 (1994).
[14] C.P. Köhler, R. Jakobi, E. Meissner, L. Wiehl, H. Spiering, P. Gütlich. *J. Phys. Chem. Solids*, **51**, 239 (1990).
[15] A.A. Soliman, M.M. Khattab, R.M. Ramadan. *Transition Met. Chem.*, **32**, 325 (2007).
[16] A. Sarkar, S. Pal. *Polyhedron*, **25**, 1689 (2006).
[17] C.M. Wilmot, C.G. Saysell, A. Blessington, D.A. Conn, C.R. Kurtis, M.J. McPherson, P.F. Knowles, S.E.V. Phillips. *FEBS Lett.*, **576**, 301 (2004).
[18] K. Takagi, T. Uehara, E. Kaneko, M. Nakayama, M. Koizumi, K. Endo, Y. Arano. *Nucl. Med. Biol.*, **31**, 893 (2004).
[19] M.N. Ackermann, K.B. Moore, A.S. Colligan, J.A. Thomas-Wohlever, K.J. Warren. *J. Organomet. Chem.*, **667**, 81 (2003).
[20] C.G. Saysell, J.M. Murray, C.M. Wilmot, D.E. Brown, D.M. Dooley, S.E.V. Phillips, M.J. McPherson, P.F. Knowles. *J. Mol. Catal. B: Enzymatic.*, **8**, 17 (2000).

[21] T. Nicholson, M. Hirsch-Kuchma, E. Freiberg, A. Davison, A.G. Jones. *Inorg. Chim. Acta*, **279**, 206 (1998).

[22] T. Nicholson, J. Cook, A. Davison, D.J. Rose, K.P. Maresca, J.A. Zubieta, A.G. Jones. *Inorg. Chim. Acta*, **252**, 421 (1996).

[23] E.C. Constable, J.M. Holmes. *Inorg. Chim. Acta*, **126**, 187 (1987).

[24] D.A. Edwards, S.J. Larter. *Polyhedron*, **5**, 1213 (1986).

[25] K. Nakamoto. *Infrared and Raman Spectra of Inorganic and Coordination Compounds*, 4th Edn, Wiley, New York (1986).

[26] M.T. Hay, B.J. Hainaut, S.J. Geib. *Inorg. Chem. Commun.*, **6**, 431 (2003).

[27] A.A. Soliman, G.G. Mohamed, W.M. Hosny, M.A. El-Mawgood. *Synth. React. Inorg. Met.-Org. Nano-Met. Chem.*, **35**, 1 (2005).

[28] C.E. Housecroft, A.G. Sharpe. *Inorganic Chemistry*, 2nd Edn, pp. 559–560, Pearson Education Limited, Essex, England (2005).

[29] R.L. Moore, R.C. Anderson. *J. Am. Chem. Soc.*, **67**, 168 (1954).

[30] S.E. Turner, R.C. Anderson. *J. Am. Chem. Soc.*, **71**, 912 (1949); W.A. Deskin. *ibid.*, **80**, 5680 (1958).

[31] S. Gangopadhyay, M. Ali. *Transition Met. Chem.*, **27**, 625 (2002).

[32] J.H. Espenson. *Chem. Kinet. React. Mech.*, 2nd Edn, p. 156, McGraw-Hill, New York (1995).